Available online at www.sciencedirect.com
SCIENCE DIRECT®
ELSEVIER
International Journal of Thermal Sciences 43 (2004) 1119–1124
International Journal of Thermal Sciences
www.elsevier.com/locate/ijts

# CFD analysis and overheating control of a turbine

Eugenio Aulisa [a], Antonio Barletta [a,*], Massimo Gallipoli [b], Alessandro Terenzi [b], Enzo Zanchini [a]

[a] *DIENCA, University of Bologna, Via dei Colli 16, 40136 Bologna, Italy*
[b] *Process Department, Snamprogetti SpA, Via Toniolo 1, 61032 Fano (PU), Italy*

Received 12 December 2003; received in revised form 31 March 2004; accepted 31 March 2004

Available online 17 June 2004

**Abstract**

The thermal analysis of a turbine stack discharging exhaust gases to the atmosphere is presented. The examined turbine stack belongs to a gas lift plant for oil extraction located in the Gulf area. The analysis has been performed because an overheating of the anchor flange/bolts and of the concrete foundation occurred and caused small cracks in the upper layer of the foundation. A qualitative thermal analysis of the stack has pointed out that the main cause of the overheating was the thermal radiation in the air-filled region underneath the stack bottom plate. Detailed calculations performed by using a CFD code (Fluent ver. 6.0.12), cross-checked with measurements taken from site, have shown that a significant reduction of the heat flux to the foundation could be obtained by filling the above mentioned air region with an insulating material. The benefits of this solution are prevailing over those achievable with the installation of external fins on the stack shell.


*Keywords:* Turbine stack; Thermal control; Computational fluid dynamics

## 1. Introduction

The operation of plants which include combustion turbines implies both noise control and thermal control problems [1]. In recent years, several noise control studies which analyze the environmental impacts of these plants have been performed [2,3]. The thermal control of steam generation in the heat recovery steam generator of a combined–cycle power plant has also been studied [4].

The aim of the analysis proposed in this paper is the determination of a method to keep the temperature of the bottom flange of a turbine stack below a given threshold value (90 °C). The importance of this thermal control is related to the need for having a very small dilation of the bottom flange, since the thermal expansion of the flange caused cracks in the concrete foundation.

A layout of the part of the turbine stack which is relevant in the study of the heat transfer with the bottom flange is given in Fig. 1. Exhaust gases with high temperature enter sideways in the steel stack and go up. Below the junction, the stack is split in two parts by an inclined steel plate; the lowest part is full of air. The stack base is welded with the steel bottom flange that is bolted in the concrete base. The

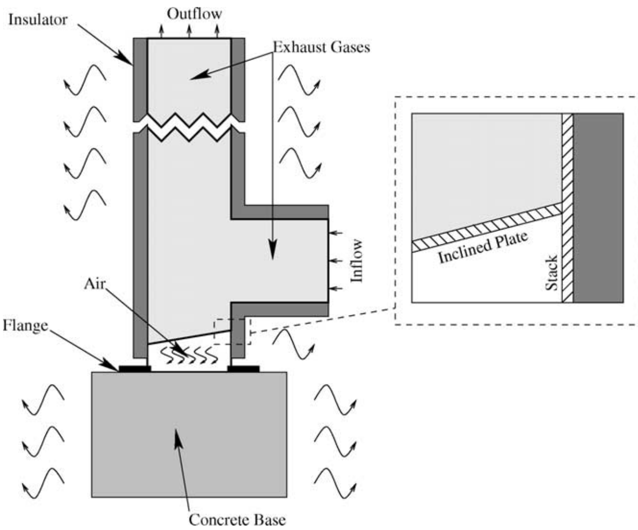


Fig. 1. Layout of the turbine stack.

* Corresponding author. Fax: +39-051-6441747.
*E-mail address:* antonio.barletta@mail.ing.unibo.it (A. Barletta).

1290-0729/$ – see front matter 
doi:10.1016/j.ijthermalsci.2004.03.005

**Nomenclature**

| | | |
|---|---|---|
| $a$ | emissivity | |
| $AEC$ | average environmental condition | |
| $C$ | dimensionless constant | |
| $CEC$ | critical environmental condition | |
| $D$ | stack diameter | m |
| $\vec{g}$ | gravitational acceleration | $m \cdot s^{-2}$ |
| $h$ | specific enthalpy | $J \cdot kg^{-1}$ |
| $h_c$ | convection coefficient | $W \cdot m^{-2} \cdot K^{-1}$ |
| $k$ | thermal conductivity | $W \cdot m^{-1} \cdot K^{-1}$ |
| $m$ | dimensionless constant | |
| $n$ | dimensionless constant | |
| $\hat{n}$ | unit normal | |
| $Nu$ | Nusselt number | |
| $p$ | static pressure | $N \cdot m^{-2}$ |
| $Pr$ | Prandtl number | |
| $q$ | heat flux | $W \cdot m^{-2}$ |
| $q_c$ | heat flux due to convection | $W \cdot m^{-2}$ |
| $q_r$ | heat flux due to radiation | $W \cdot m^{-2}$ |
| $Re$ | Reynolds number | |
| $T$ | temperature | °C |
| $T_e$ | external temperature | °C |
| $T_{in}$ | inlet temperature | °C |
| $\vec{u}$ | velocity field | $m \cdot s^{-1}$ |
| $U_{in}$ | inlet velocity magnitude | $m \cdot s^{-1}$ |
| $V$ | undisturbed air speed | $m \cdot s^{-1}$ |

*Greek symbols*

| | | |
|---|---|---|
| $\mu$ | dynamic viscosity | $kg \cdot m^{-1} \cdot s^{-1}$ |
| $\nu$ | kinematic viscosity | $m^2 \cdot s^{-1}$ |
| $\rho$ | density | $kg \cdot m^{-3}$ |
| $\sigma_0$ | Stephan–Boltzmann constant, $= 5.672 \times 10^{-8}\ W \cdot m^{-2} \cdot K^{-4}$ | |

*Subscripts*

| | |
|---|---|
| $D$ | referred to the diameter |
| $S$ | referred to the surface |

stack is covered by insulating material (rockwool) for one third of its height.

The examined turbine stack belongs to a gas lift plant (i.e., a plant injecting gas into wells to get crude oil) located in the Gulf area. The working conditions, the material properties and the environmental conditions are known; moreover temperature measurements on the external surface of the bottom flange and of the concrete base have been performed.

The main heat transfer mechanisms in the system examined are as follows. The exhaust gases heat the upper part of the stack and the inclined steel plate by convection heat transfer. The lowest part of the stack, the bottom flange and the upper layer of the concrete base are heated by conduction through the stack wall, as well as by convection and radiation through the internal air layer. Heat is transferred to the external environment, by convection and radiation, through the external surfaces of the stack.

First, a qualitative thermal analysis of the stack has been performed. This analysis has pointed out that the main cause of the temperature increase of the bottom flange and of the concrete base is the radiation heat transfer between the inclined internal steel plate and the upper surface of the concrete base. Indeed, the air layer between these surfaces has a very low thermal conductivity, undergoes a negligible free convection flow, but is transparent to thermal radiation. As a consequence, the replacement of this air layer with an opaque insulating material appears as necessary. The axial heat conduction in the wall of the stack yields a non-negligible contribution to the temperature increase of the bottom flange. This contribution can be significantly reduced by removing a portion of the external rockwool layer. The enhancement of the external heat transfer by means of fins placed on the wall of the vertical tube should yield a minor contribution to the thermal control of the bottom flange.

The qualitative thermal analysis has been validated by means of numerical simulations of the heat transfer process. These simulations have been performed by using a CFD code (Fluent ver. 6.0.12). The main steps of the analysis are the following:

(1) estimate of reasonable convection and radiation coefficients necessary to impose thermal boundary conditions;
(2) discretization of the computational domain and CFD modelling;
(3) thermal analysis of the existing system and comparison of results with experimental data;
(4) analysis under critical conditions of the combined effect due to the addition of internal opaque insulating material and to the removal of a portion of the external rockwool layer;
(5) study of the effect due to an additional array of circular pin fins placed on the external surface of the tube.

## 2. Estimate of convection and radiation coefficients

The convection coefficient $h_c$ for the heat transfer from the external surface of the stack to external air has been evaluated as

$$h_c = \frac{k}{D}\overline{Nu}_D \tag{1}$$

where $k$ is the thermal conductivity of the external air, $D$ is the diameter of the stack and $\overline{Nu}_D$ is the circumferentially averaged Nusselt number. With reference to transverse flow around an infinitely long cylinder, $\overline{Nu}_D$ has been estimated by means of Zhukauskas' correlation [5],

$$\overline{Nu}_D = C Re_D^m Pr^n \left(\frac{Pr}{Pr_S}\right)^{1/4} \tag{2}$$

where $n$ is a dimensionless constant which depends on the Prandtl number $Pr$, while $C$ and $m$ are dimensionless constants which depend on the Reynolds number $Re_D$. The latter is defined as

$$Re_D = \frac{VD}{\nu} \tag{3}$$

where $V$ is the undisturbed air speed and $\nu$ is the kinematic viscosity of air. All physical properties are evaluated at the external air temperature [6], except $Pr_S$, which is evaluated at the mean temperature on the external surface of the stack. For air, the Prandlt number is a constant with value 0.71. Therefore, $n = 0.37$ and Eq. (2) reduces to

$$\overline{Nu}_D = 0.88 C\, Re_D^m \tag{4}$$

The stack diameter is $D = 2.4$ m.

The external convection coefficient has been evaluated in two different conditions:

*Average Environmental Condition (AEC).* The wind speed corresponds to the arithmetic mean of the measured values, 3.0 $\mathrm{m \cdot s^{-1}}$; the external-air temperature corresponds to the arithmetic mean of the measured values, 42 °C;

*Critical Environmental Condition (CEC).* The wind speed is very low, 0.2 $\mathrm{m \cdot s^{-1}}$; the external-air temperature is 50 °C.

In both cases, the mean temperature on the external surface of the stack has been assumed equal to 100 °C. Under these conditions, the results are as follows:

$$\begin{aligned} &AEC \rightarrow \overline{Nu}_D = 577 \rightarrow h_c = 6.56\ \mathrm{W \cdot m^{-2} \cdot K^{-1}} \\ &CEC \rightarrow \overline{Nu}_D = 102 \rightarrow h_c = 1.15\ \mathrm{W \cdot m^{-2} \cdot K^{-1}} \end{aligned} \tag{5}$$

The external radiation heat transfer coefficient has been evaluated by assuming an emissivity 0.8 for the stack–skirt (smoked) steel as well as for the concrete surface, and an emissivity 0.2 for the external surface of the thermal insulation. The thermal radiation heat transfer between the inclined internal steel plate and the concrete base has been evaluated with an emissivity 0.8 of both surfaces.

## 3. CFD modelling

### 3.1. The computational domain

In Fig. 2, a drawing of the computational domain and of its mesh is reported, with reference to the existing system. The upper surface of the concrete base has been assumed as the zero-height plane. A part of the vertical tube, up to the height of 5.0 m, has been selected, together with a part of the lateral inlet pipe with length 3.0 m. Both ducts have been considered as constant-section circular tubes with a diameter of 2.4 m. The height of the inlet-pipe bottom has been considered equal to 1.125 m. Starting from the bottom flange, a 0.20 m high portion of the vertical tube is free of insulation. Then, in a 0.80 m high portion of the vertical tube, the thermal insulation has been modelled as a 0.20 m thick layer around the tube. In the upper part of the computational domain, the thermal insulation has been taken into account through the thermal boundary condition. The inclined steel plate has been considered with a minimum height of 0.51 m and a maximum height of 0.64 m. The bottom flange is a circular ring 0.035 m thick with an internal diameter and an external diameter of 2.4 m and 2.7 m, respectively. The concrete base has been modelled as a box with a square section of 3.5 m × 3.5 m and a height of 1.7 m; its bottom surface has been assumed adiabatic. The number of nodes in the mesh is 46036.

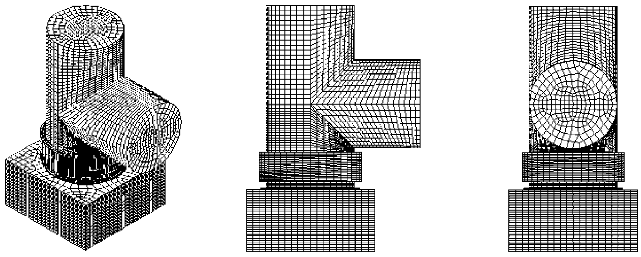

Fig. 2. Computational domain of the existing system.

### 3.2. Governing equations

In this section the physical assumptions, used to investigate the stack system, are briefly discussed. Non-isothermal, incompressible flows have been considered in both parts of the stack, although in the closed region under the inclined steel plate the flow is assumed to be laminar while in the upper part it is assumed to be turbulent. The conservation equations for mass, momentum and energy for incompressible flows have been solved in both regions. The equation for the mass conservation, or continuity equation, can be written as

$$\nabla \cdot \vec{u} = 0 \tag{6}$$

where $\vec{u}$ is velocity field. The equation for the momentum conservation in an inertial reference system is described by

$$\frac{\partial}{\partial t}(\rho \vec{u}) + \nabla \cdot (\rho \vec{u}\vec{u}) = -\nabla p + \nabla \cdot (\mu \nabla \vec{u}) + \rho \vec{g} \tag{7}$$

where $\rho$ is the density, $p$ is the static pressure, $\mu$ is the molecular viscosity and $\rho\vec{g}$ is the gravitational body force. The energy equation is solved in the following form:

$$\frac{\partial}{\partial t}\left[\rho\left(h + \frac{u^2}{2}\right)\right] + \nabla \cdot \left\{\vec{u}\left[\rho\left(h + \frac{u^2}{2}\right) + p\right]\right\} = \nabla \cdot (k \nabla T) \tag{8}$$

where $h$ is the specific enthalpy, $k$ is the thermal conductivity and $T$ is the temperature. Internal thermal radiation heat transfer has been taken into account in the closed region under the plate only between the inclined steel plate and the concrete base.

Turbulent flows are characterized by fluctuating velocity fields. These fluctuations mix the transported quantities such as momentum and energy and can be of small scale and high frequency. Therefore turbulent flows are too computationally expensive to be simulated directly in practical calculations. On the other hand, the instantaneous exact governing equations (6)–(8) can be averaged in time and in space or otherwise manipulated to remove these small scales, resulting in a modified set of equations that are computationally less expensive to solve. However, the modified equations contain additional unknown variables. Then, additional turbulence equations are needed to determine these variables in terms of known quantities. The standard $k$–$\varepsilon$ model, proposed by Launder and Spalding [7], has been chosen. It is a semi-empirical model, and the derivation of the model equations relies on phenomenological considerations. It is based on model transport equations for the turbulence kinetic energy, $k$, and its dissipation rate, $\varepsilon$.

In the solid regions, only the energy equation has been solved, by using the following form

$$\frac{\partial}{\partial t}(\rho h) = \nabla \cdot (k \nabla T) \tag{9}$$

### 3.3. Boundary conditions

The system of conservation equations must be supplemented with appropriate boundary conditions. Fig. 3 shows separately the boundary conditions for the energy equation (left) and for the continuity and the momentum equations (right). The value $T_{\text{in}}$ is the temperature of the inlet flow, $T_{\hat{n}_2}$ is the partial derivative of $T$ along the normal $\hat{n}_2$, and $q$ is the heat flux per unit area. The heat fluxes $q_c$ and $q_r$ are due to the convection and radiation, respectively. They have been evaluated in the following form

$$q_c = h_c(T - T_e) \tag{10}$$

$$q_r = a\sigma_0\left(T^4 - T_e^4\right) \tag{11}$$

where $T_e$ is the external temperature, $a$ is the emissivity of the surface and $\sigma_0$ is the Stephan–Boltzmann constant. In Fig. 3 $U_{\text{in}}$ is the magnitude of the velocity component normal to the inlet surface and $\vec{u}_{\hat{n}_2}$ is the partial derivative of $\vec{u}$ evaluated along the normal $\hat{n}_2$. According with Launder and Spalding [7], turbulent kinetic energy and its dissipation rate have been chosen to be constant and unitary on all the open boundaries.

### 3.4. Numerical algorithms

The numerical algorithm adopted in the stack simulation is as follows. A segregated solver has been used, where the governing equations of Section 3.2 are discretized with a control-volume-based technique and are solved sequentially.

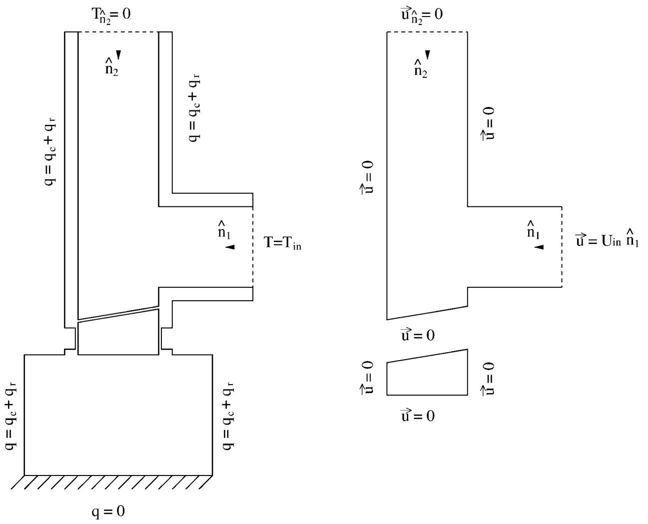


Fig. 3. Boundary conditions of the existing system.

The set of non-linear governing equations is linearized and a stationary solution is considered. Velocity field components are first evaluated and then a "Poisson-type" equation for the pressure is solved to obtain a correction for the pressure, in order to satisfy the continuity and momentum equations. Turbulence and temperature equations are then solved using the updated values of other variables. Due to the non-linearity of all the equations, this loop is repeated until convergence is achieved. Scalar variables, including the velocity components, are located at cell center and their value at cell faces is obtained with a second-order upwind scheme. All equations are solved with an Algebraic Multigrid (AMG) technique, in particular a fixed V-cycle has been adopted for the Poisson's equation for the pressure and a Flexible cycle for the other transport equations. Under-relaxation factors have been considered to control the change of the physical variables during each iteration.

## 4. CFD analysis of the existing system

The thermal behavior of the existing system has been simulated numerically under average environmental conditions (*AEC*), in order to check whether the model yields the measured temperature values at the bottom flange, as well as under critical environmental conditions (*CEC*). Under *AEC*, the external convection coefficient is 6.56 $\text{W}\cdot\text{m}^{-2}\cdot\text{K}^{-1}$, the external air temperature is 42 °C. Moreover, under *AEC* the inlet temperature of exhaust gases is 500 °C, i.e., the temperature of the exhaust gases under normal operating conditions of the gas lift plant. Under *CEC*, the external convection coefficient is 1.15 $\text{W}\cdot\text{m}^{-2}\cdot\text{K}^{-1}$, the external air temperature is 50 °C and the inlet temperature of exhaust gases is 580 °C. The latter is the highest temperature that the exhaust gases can reach. The inlet velocity magnitude of the gas is 11 $\text{m}\cdot\text{s}^{-1}$ in both cases. The main results of the numerical simulations are reported in Table 1 and in Figs. 4 and 5. The mean temperature of the bottom flange under *AEC* is in fair agreement with the arithmetic mean of the measured values (172 °C). The temperature of the upper surface of the concrete base reported in Table 1 is the temperature of the concrete upper surface internal to the vertical tube. The table shows that under *CEC* the concrete temperature can reach 343 °C, while the local temperature of the surface of the bottom flange can reach 240 °C. A qualitative structural analysis reveals that both the bottom flange dilation and the very high temperature of the concrete base may be causes of cracks.

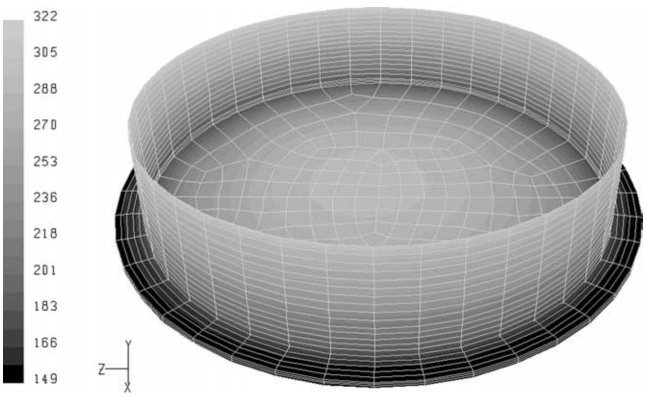


Fig. 4. Temperature map of the bottom part of the stack under *AEC*.

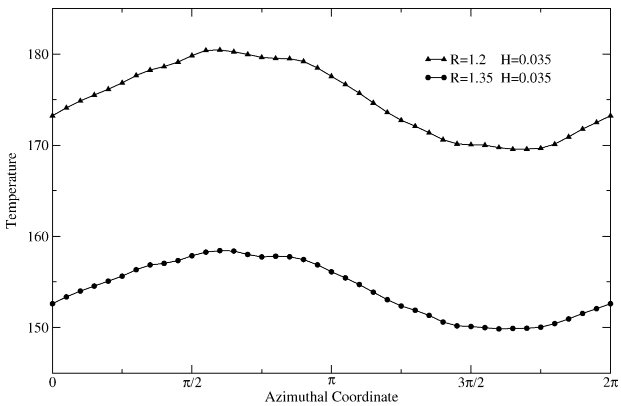


Fig. 5. Temperature of the bottom flange under *AEC*.

Table 1
Temperature values of the existing system

| Region | Temperature °C | | |
|---|---|---|---|
| | Min | Mean | Max |
| AEC | | | |
| Bottom flange | 149 | 166 | 185 |
| Upper surface of the concrete base | 178 | 255 | 286 |
| CEC | | | |
| Bottom flange | 198 | 211 | 240 |
| Upper surface of the concrete base | 224 | 298 | 343 |

## 5. CFD analysis of the modified system

In the existing system, the most important heat transfer contribution from the hot exhaust gases to the concrete base and to the bottom flange occurs through the air layer below the inclined steel plate. The prevalent heat transfer mechanism in this layer is thermal radiation. Therefore, the system has been modified by filling this layer with a low-conductivity opaque material (vermiculite, 0.1 $W \cdot m^{-1} \cdot K^{-1}$). Then, in order to reduce the thermal conduction through the steel wall of the stack, the lowest part of the external rockwool layer, from the height of 0.20 m to the height of 1.0 m, has been removed. Thus, the modified computational domain can been obtained from that described in Section 3.1 by removing the insulation layer geometrically modelled. Numerical computations have been performed under critical environmental conditions, *CEC*. The main results are reported in Table 2 and in Figs. 6 and 7. The mean tem-

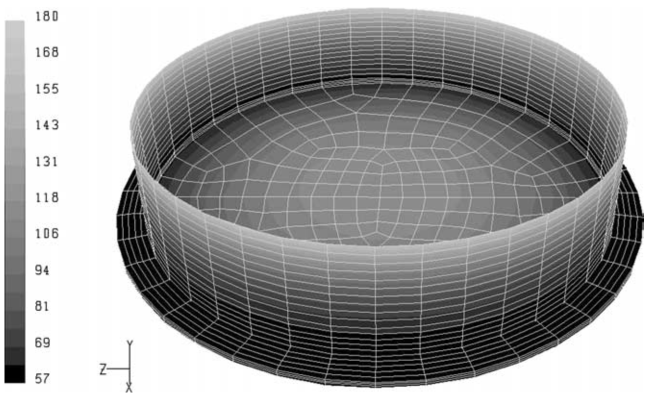


Fig. 6. Temperature map of the bottom part of the stack under *CEC*.

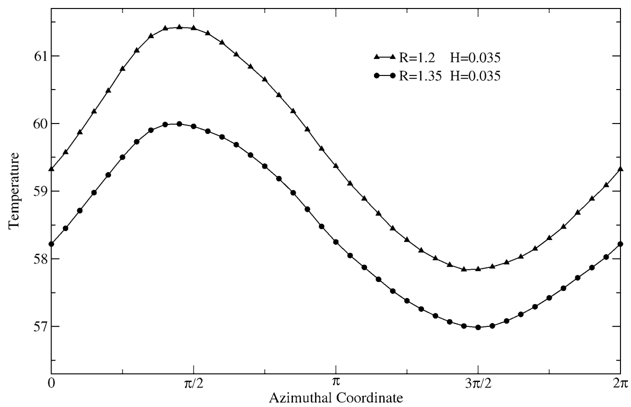


Fig. 7. Temperature of the bottom flange under *CEC*.

Table 2
Temperature values of the modified system under *CEC*

| Region | Temperature °C | | |
|---|---|---|---|
| | Min | Mean | Max |
| Bottom flange | 56 | 58 | 61 |
| Upper surface of the concrete base | 59 | 91 | 118 |

perature of the bottom flange is 58 °C, and the maximum temperature thereof is much lower than 90 °C. Moreover, the temperatures of the upper surface of the concrete base are much lower than those obtained in the previous case (existing system under *CEC*).

## 6. Effect of pin fins on the modified system

The effect of external pin fins, in addition to the insertion of an internal layer of insulating material (vermiculite) and to the removal of the lowest part of the external rockwool layer, has been analyzed under *CEC*. A row of 48 inclined steel pin fins, with a slope of 45°, has been considered. Each fin has a length of 0.28 m, a diameter of 0.03 m, and is placed on the wall of the tube at a height of 0.18 m from the upper surface of the concrete base. In order to limit the number of nodes in the mesh (about 69000 nodes), the computational domain has been reduced. Indeed, only a circular sector (30° wide) has been considered, with a height of 0.57 m with respect to the upper surface of the concrete base. The reduced computational domain, together with a detail of the mesh, is depicted in Fig. 8. Under critical environmental conditions (*CEC*), the external convection coefficient is 1.15 $\mathrm{W{\cdot}m^{-2}{\cdot}K^{-1}}$ and the external air temperature is 50 °C. The inclined steel plate has been assumed as isothermal, with a temperature of 580 °C, while all the other new surfaces, obtained reducing the domain, have been considered as adiabatic ($q = 0$). In Table 3, the temperatures of the bottom flange evaluated in the presence of the external pin fins are compared with those obtained in the absence of fins. The results reveal that the addition of external pin fins to the modified system yields a very small change of the temperatures of the bottom flange.

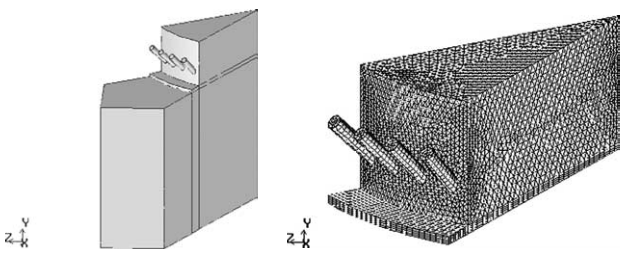

(a) (b)

Fig. 8. Reduced computational domain (a) and mesh of the upper part thereof (b).

Table 3
Temperature values comparison under *CEC*

| Region | Temperature °C | | |
|---|---|---|---|
| | Min | Mean | Max |
| Bottom flange (system with fins) | 56 | 61 | 65 |
| Bottom flange (system without fins) | 57 | 63 | 68 |

## 7. Conclusions

A turbine stack discharging exhaust gases to the atmosphere has been simulated in severe operating conditions. The technical solution which has been proposed and adopted is effective in eliminating critical thermal effects. The decrease of the bottom-flange temperature has been obtained by filling the air layer with vermiculite. This decrease has been predicted through CFD calculations performed by Fluent software. The thermal analysis has suggested the optimal remedial action both in terms of economics and of impact on the system. The analysis has also allowed one to reject the installation of pin fins on the stack external surface, that would have caused considerable welding and bulkiness troubles. The proposed solution has been applied. Measurements performed on the modified system have confirmed the effectiveness of the solution and the accuracy of the predictions obtained by means of the CFD code.

## References


[1] 30th GENERAL ELECTRIC Industrial Gas Turbine State of the Art Seminar, Saratoga Springs, New York, 1982.

[2] L.A. Beeson, G.A. Schott, Experience with active control of exhaust noise from a large frame combustion turbine, in: Proceedings of the 1997 International Gas Turbine & Aeroengine Congress & Exposition, Orlando, Florida, USA, 1997, ASME Paper 97-GT-139.

[3] D.J. Parzych, S.A. Youtt, Experimental investigation of combustion turbine exhaust stack silencer performance, in: Proceedings of the National Conference on Noise Control Engineering, Ypsilanti, USA, 1998, pp. 211–216.

[4] S.Z. Akhtar, Proper steam bypass system design avoids steam turbine overheating, Power Engineering (Barrington, Illinois) 107 (2003) 44–52.

[5] F.P. Incropera, P. De Witt, Fundamentals of Heat and Mass Transfer, Wiley, New York, 1985.

[6] K. Raznjevic, Handbook of Thermodynamic Tables, Begell House, New York, 1995.

[7] B.E. Launder, D.B. Spalding, The numerical computation of turbulent flows, Comput. Methods Appl. Mech. Engrg. 3 (1974) 269–289.